Thermally activated delayed fluorescence organic dots for two-photon fluorescence lifetime imaging

Tingchao He,[1] Can Ren,[1] Zhuohua Li,[2] Shuyu Xiao,[1] Junzi Li,[1] Xiaodong Lin,[1] Chuanxiang Ye,[1] Junmin Zhang,[2,a)] Lihong Guo,[3] Wenbo Hu,[3,a)] and Rui Chen[4]
[1]*College of Physics and Energy, Shenzhen University, Shenzhen 518060, China*
[2]*College of Chemistry and Environmental Engineering, Shenzhen University, Shenzhen 518060, China*
[3]*Key Laboratory of Flexible Electronics (KLOFE) and Institute of Advanced Materials (IAM), Jiangsu National Synergetic Innovation Center for Advanced Materials (SICAM), Nanjing Tech University (NanjingTech), 30 South Puzhu Road, Nanjing 211800, China*
[4]*Department of Electrical and Electronic Engineering, Southern University of Science and Technology, Shenzhen 518055, China*

(Received 11 April 2018; accepted 9 May 2018; published online 21 May 2018)

Autofluorescence is a major challenge in complex tissue imaging when molecules present in the biological tissue compete with the fluorophore. This issue may be resolved by designing organic molecules with long fluorescence lifetimes. The present work reports the two-photon absorption (TPA) properties of a thermally activated delayed fluorescence (TADF) molecule with carbazole as the electron donor and dicyanobenzene as the electron acceptor (i.e., 4CzIPN). The results indicate that 4CzIPN exhibits a moderate TPA cross-section ($\sim 9 \times 10^{-50}$ cm^4 s photon^{-1}), high fluorescence quantum yield, and a long fluorescence lifetime (~ 1.47 μs). 4CzIPN was compactly encapsulated into an amphiphilic copolymer via nanoprecipitation to achieve water-soluble organic dots. Interestingly, 4CzIPN organic dots have been utilized in applications involving two-photon fluorescence lifetime imaging (FLIM). Our work aptly demonstrates that TADF molecules are promising candidates of nonlinear optical probes for developing next-generation multiphoton FLIM applications. *Published by AIP Publishing.* https://doi.org/10.1063/1.5034375

Recently, fluorescence lifetime imaging (FLIM) has attracted significant attention as it enables elimination of short-lived background fluorescence and provides high signal-to-noise ratios.[1] To date, considerable efforts have focused on developing suitable emissive probes, with long-lived fluorescence lifetimes, which may be used in FLIM.[2–4] Among the various emissive materials, phosphorescent materials are the most important probes in FLIM because of their relatively long lifetimes, with some in the order of seconds.[5,6] However, the application of phosphorescent materials in FLIM is limited by their relatively weak phosphorescence and concerns about unknown long-term toxicity caused by heavy metals present in such materials. Therefore, efforts should focus on developing pure organic molecules with long-lived fluorescence lifetimes, ultrabright emission, and biocompatibility for FLIM applications.

Although numerous fluorescent dyes have been reported to be nontoxic to cells, most suffer from the limitation of short fluorescence lifetimes (in the nanosecond range).[7,8] Therefore, conventional organic dyes cannot overcome most autofluorescent backgrounds in biological systems. To extend the lifetime of fluorescent dyes and avoid the toxic effects of heavy-metal complexes on cells, organic fluorescent dyes with long fluorescence lifetimes are highly desirable. Adachi *et al.* reported a thermally activated delayed fluorescence (TADF) mechanism for realizing efficient organic light-emitting diodes.[9] TADF molecules undergo efficient reverse intersystem crossing (RISC) from a triplet excited state to a singlet state. As a result, these molecules generally exhibit ultrahigh fluorescence quantum efficiency Φ and ultralong fluorescence lifetimes, both of which are extremely useful for FLIM. For example, a fluorescein derivative and 2,3,5,6-tetracarbazole-4-cyano-pyridine-based organic dots have been used for FLIM in living cells (i.e., *in vivo*).[10,11] The self-assembly of TADF molecules into large organic dots can combine the advantages of both small molecules and large nanoparticles for *in vivo* bioimaging. On one hand, the small molecular probe has deep-tissue penetration and ideal biodistribution. On the other hand, large organic dots lead to increased residence time in the target tissue of interest such as tumor.[12] However, these TADF probes were designed based on one-photon FLIM. Compared with one-photon FLIM, two-photon FLIM has significant advantages in terms of higher spatial resolution, deeper penetration depth, and lower phototoxicity.[13–15] However, the relevant studies on two-photon FLIM of TADF organic dots are rare and remain to be challenging.

In the present work, we synthesized the TADF molecule 4CzIPN, which comprises carbazole as the electron donor and dicyanobenzene as the electron acceptor.[9] The maximum two-photon absorption (TPA) cross-section of 4CzIPN was measured to be 9 GM (where 1 GM $= 10^{-50}$ cm^4 s photon^{-1}), and its fluorescence lifetime was up to 1.47 μs, which is comparable to that of luminescent pincer platinum(II) complexes.[3] Two-photon FLIM results show that 4CzIPN organic dots are internalized in cells and can efficiently eliminate autofluorescence from molecules in biological tissue.

The chemical structure of 4CzIPN is presented in Fig. 1(a). Figure 1(b) shows the normalized absorption and fluorescence spectra of 4CzIPN in organic solvents of differing polarity

a)Authors to whom correspondence should be addressed: zhangjm@szu.edu.cn and iamwbhu@njtech.edu.cn

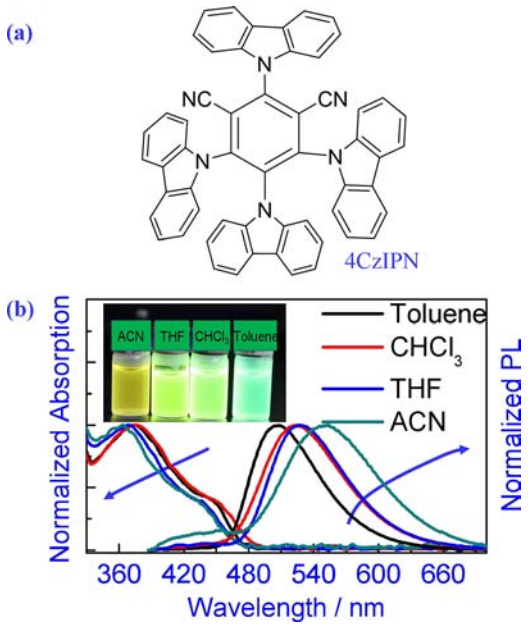

FIG. 1. (a) Chemical structure of 4CzIPN. (b) Normalized absorption and fluorescence spectra of 4CzIPN in various solvents.

[i.e., toluene, chloroform ($CHCl_3$), tetrahydrofuran (THF), and acetonitrile (ACN)]. The absorption bands of 4CzIPN are blue shifted when changing from low- to high-polarity organic solvents. The observed negative solvatochromism is related to the solute-solvent electrostatic interaction due to the molecular symmetric structure.[16] The peak emission wavelengths were measured to be 507, 524, 527, and 551 nm for 4CzIPN in toluene, $CHCl_3$, THF, and ACN, respectively. The fluorescence peak clearly red shifts with the increasing polarity of the organic solvent. The redshift of the emission peak is attributed to the charge-transfer properties of the solvent-relaxed emissive state.[17]

Figure 1(b) shows that negligible linear absorption occurs in 4CzIPN from 500 to 900 nm, making it suitable for two-photon excitation. As expected, upon excitation at 800 nm, bright fluorescence still appears, and fluorescence emission spectra are readily detected [Fig. 2(a)]. To confirm that the fluorescence of 4CzIPN is indeed induced by two-photon excitation, its relative emission intensity was measured as a function of the excitation power at 800 nm. The data are well fit by a straight line on a logarithmic scale with a slope of about two, indicating the quadratic dependence on excitation power predicted by TPA theory [Fig. 2(b)].[18]

From an application viewpoint, elucidation of the TPA spectrum for 4CzIPN is important as it determines the most efficient wavelengths for two-photon excitation. The TPA cross-section σ_2 of 4CzIPN was therefore measured at various wavelengths using the *Z*-scan technique.[19] Based on the analysis of σ_2 as a function of the wavelength, we find that the peak TPA band appears to be significantly blue shifted with respect to twice the energy of the low-energy peak in the one-photon-absorption spectrum. The blueshift of the TPA peak is attributed to the different selection rules for one- and two-photon transitions.[20] The TPA cross-sections for 4CzIPN in toluene, $CHCl_3$, THF, and ACN were measured to be 5, 7, 9, and 4 GM, respectively. Additionally, the

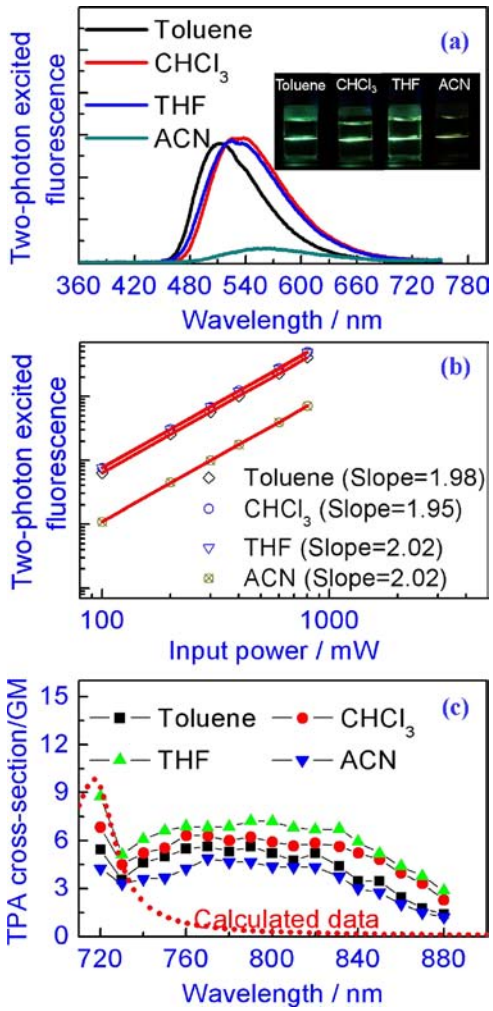

FIG. 2. (a) Two-photon-excited fluorescence spectra of 4CzIPN excited at 800 nm, and the spectral intensity is relative; the inset shows a photograph of the fluorescence from the 4CzIPN solution. (b) Two-photon-excited fluorescence intensity as a function of excitation power. (c) Experimental TPA spectra of 4CzIPN in various solvents and the calculated TPA spectrum. In the measurements, the same concentration ($\sim 1 \times 10^{-4}$ M) is used for all the solutions.

TPA spectrum of 4CzIPN was calculated using modern analytical response theory as implemented in the Dalton software package, with the exchange-correlation functional B3LYP and the basis set 6–31G.[21] The calculated TPA cross-sections are in the same order of magnitude compared to the experimental results. Since the solvent influences have not been taken into consideration in the calculation process, the wavelength dispersion of calculated TPA cross-sections is different with respect to experimental results.

Because the steric hindrance between the carbazole and dicyanobenzene moieties leads to a large dihedral angle of about 60° between the planes of the carbazole and dicyanobenzene groups,[11] the nonplanar structure of 4CzIPN is considered undesirable for enhancing TPA.[22] As a result, 4CzIPN exhibits relatively small TPA in the measured spectral range. Two-photon brightness (or the action cross-section, $\sigma_2 \cdot \Phi$) is an important parameter for practical bioimaging applications. The two-photon brightness of 4CzIPN in toluene, $CHCl_3$, THF, and ACN was determined to be 4.7, 5.7, 5.6, and 0.8 GM, respectively. Although the TPA cross-sections of 4CzIPN in the various solvents are relatively

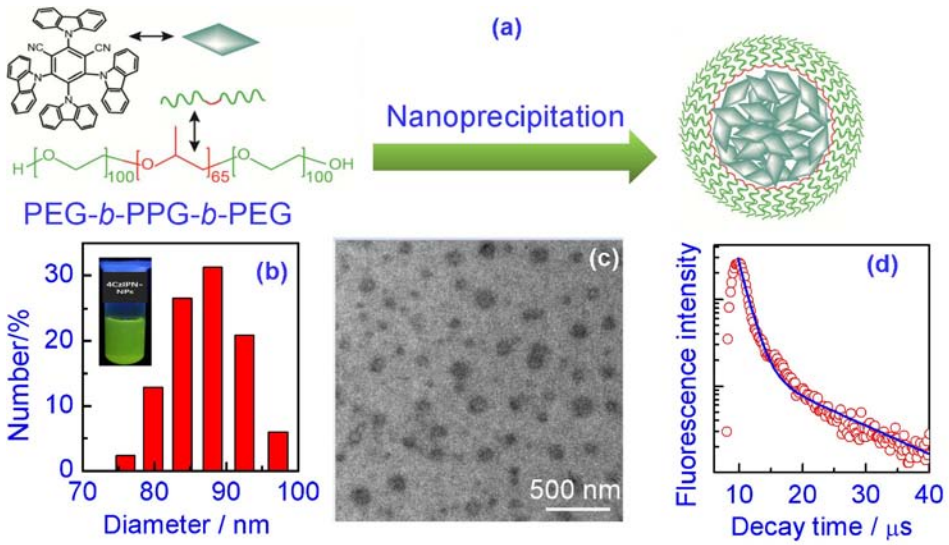

FIG. 3. (a) Schematic illustration of 4CzIPN organic dots prepared by nanoprecipitation. (b) Dynamic light scattering and (c) transmission electron microscopy images of 4CzIPN organic dots. The inset of panel (b) shows a photograph of the fluorescence 4CzIPN organic dots. (d) Fluorescence lifetime of organic dots in water in ambient atmosphere (300 K in air, excited at 405 nm, and fluorescence collected at 550 nm); the time resolution in the measurement of delayed fluorescence lifetime is ~100 ns.

small, its two-photon brightness is still moderate and comparable to that of curcumin[23] and Ir(III)-complex-based phosphorescent polymer dots.[24] We therefore conclude that the high fluorescence quantum yield of 4CzIPN largely compensates for the decrease in two-photon brightness caused by the nonplanar molecular structure.

To further enhance the biocompatibility of 4CzIPN in living cells, stable 4CzIPN organic dots in aqueous solutions were formulated using the nanoprecipitation method, where a THF solution containing an amphiphilic copolymer (PEG-b-PPG-b-PEG) and 4CzIPN was quickly injected into water under sonication [Fig. 3(a)]. THF was then removed through natural volatilization to obtain water-soluble 4CzIPN organic dots. The results of dynamic light scattering indicate that organic dots have a relatively narrow size distribution with an average hydrodynamic size of 88 nm [Fig. 3(b)]. Furthermore, 4CzIPN organic dots were found to exhibit bright fluorescence upon irradiation by ultraviolet light [see the inset of Fig. 3(b)]. Transmission electron microscopy images indicate that the organic dots possess a spherical morphology [Fig. 3(c)]. 4CzIPN organic dots exhibit double-exponential fluorescence decay behavior. The prompt component, which is attributed to the direct fluorescence emission from the S_1 state to the S_0 state of 4CzIPN organic dots, was measured to be ~3.9 ns by using a time-correlated single-photon counting (TCSPC) technique at 25 °C in air. Additionally, the delayed component of the organic dots, which is attributed to delayed fluorescence occurring via RISC, was also measured using a TCSPC technique [Fig. 3(d)]. The weighted-average lifetime of delayed fluorescence is calculated to be 1.47 μs, which is sufficiently long as compared to that of these short-lived endogenous dyes (on the order of hundred-picosecond to several nanoseconds) for FLIM.[25]

To demonstrate the imaging ability of 4CzIPN in living cells, fluorescence images of HeLa cells inculcated with 4CzIPN organic dots (20 μM) were obtained from traditional two-photon confocal fluorescence imaging and two-photon FLIM. As shown in Fig. 4(a), two-photon confocal fluorescence imaging shows that 4CzIPN organic dots readily enter the cytoplasm and exhibit strong fluorescence. The intensity of two-photon FLIM reveals that the signals are evenly distributed across the cytoplasm [Fig. 4(b)], which was consistent with the result of two-photon confocal fluorescence imaging. The lifetime map reveals that the lifetime of 4CzIPN organic

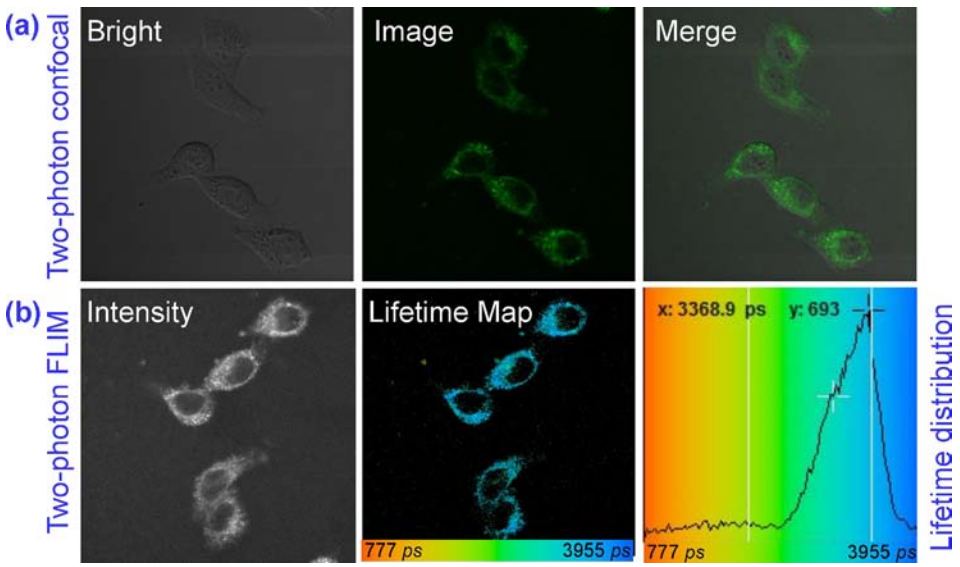

FIG. 4. (a) Two-photon confocal fluorescence images of HeLa cells incubated with 4CzIPN organic dots; from left to right: bright-field imaging of HeLa cells, dark-field imaging of HeLa cells incubated with 4CzIPN organic dots, and overlay of bright-field imaging and dark-field imaging. (b) Two-photon FLIM of HeLa cells incubated with 4CzIPN (20 μM); from left to right: fluorescence intensity, life-time map, and life-time distribution. The excitation wavelength is 800 nm, and lifetime signals were recorded at 480–600 nm.

dots is mainly distributed over a wide range from ~2000 to 4000 ps in the cellular environment. More importantly, the signals from short-lived autofluorescence were remarkably reduced. It should be noted that the time delay could not go to a much longer regime (~ms) due to the high repetition of femtosecond pulses (~80 MHz) used in the FLIM. Even so, the experimental results presented here still can confirm that the 4CzIPN organic dots are promising for applications involving two-photon FLIM.

In conclusion, we report the TPA properties of a TADF molecule with carbazole as the electron donor and dicyanobenzene as the electron acceptor. By exploiting its reasonable TPA cross-section, high fluorescence quantum yield, and long fluorescence lifetime, organic dots based on this TADF molecule may be used in two-photon FLIM applications. We believe that TADF molecules may enable fresh probes for next-generation multiphoton FLIM applications.

This work was financially supported by the National Natural Science Foundation of China (11404219), the Shenzhen Basic Research Project of Science and Technology (JCYJ20170302142433007 and KQTD2015071710313656), the Natural Science Foundation of Jiangsu Province of China (BK20171020), China Postdoctoral Science Foundation (2017M621733), and Natural Science Foundation of SZU (827-000069).

[1]K. Y. Zhang, Q. Yu, H. Wei, S. Liu, Q. Zhao, and W. Huang, Chem. Rev. **118**, 1770 (2018).
[2]N. Takahashi, W. Sawada, J. Noguchi, S. Watanabe, H. Ucar, A. Hayashi-Takagi, S. Yagishita, M. Ohno, H. Tokumaru, and H. Kasai, Nat. Commun. **6**, 8531 (2015).
[3]P. Chow, G. Cheng, G. S. Tong, W. To, W. Kwong, K. Low, C. Kwok, C. Ma, and C. Che, Angew. Chem., Int. Ed. **54**, 2084 (2015).
[4]T. He, J. Li, C. Ren, S. Xiao, Y. Li, R. Chen, and X. Lin, Appl. Phys. Lett. **111**, 211105 (2017).
[5]M. Delbianco, V. Sadovnikova, E. Bourrier, G. Mathis, L. Lamarque, J. M. Zwier, and D. Parker, Angew. Chem., Int. Ed. **53**, 10718 (2014).
[6]Z. Chen, K. Y. Zhang, X. Tong, Y. Liu, C. Hu, S. Liu, Q. Yu, Q. Zhao, and W. Huang, Adv. Funct. Mater. **26**, 4386 (2016).
[7]T. He, S. Yao, J. Zhang, Y. Li, X. Li, J. Hu, R. Chen, and X. Lin, Opt. Express **24**, 11091 (2016).
[8]D. Li, P. Jing, L. Sun, Y. An, X. Shan, X. Lu, D. Zhou, D. Han, D. Shen, Y. Zhai, S. Qu, R. Zbořil, and A. L. Rogach, Adv. Mater. **30**, 1705913 (2018).
[9]X. Xiong, F. Song, J. Wang, Y. Zhang, Y. Xue, L. Sun, N. Jiang, P. Gao, L. Tian, and X. Peng, J. Am. Chem. Soc. **136**, 9590 (2014).
[10]T. T. Li, D. L. Yang, L. Q. Zhai, S. L. Wang, B. M. Zhao, N. N. Fu, L. H. Wang, Y. T. Tao, and W. Huang, Adv. Sci. **4**, 1600166 (2017).
[11]H. Uoyama, K. Goushi, K. Shizu, H. Nomura, and C. Adachi, Nature (London) **492**, 234 (2012).
[12]K. Pu, J. Mei, J. V. Jokerst, G. Hong, A. L. Antaris, N. Chattopadhyay, A. J. Shuhendler, T. Kurosawa, Y. Zhou, S. S. Gambhir, Z. Bao, and J. Rao, Adv. Mater. **27**, 5184 (2015).
[13]S. Lu, L. Sui, J. Liu, S. Zhu, A. Chen, M. Jin, and B. Yang, Adv. Mater. **29**, 1603443 (2017).
[14]T. He, Y. Gao, S. Sreejith, X. Tian, L. Liu, Y. Wang, H. Joshi, S. Z. F. Phua, S. Yao, X. Lin, Y. Zhao, A. C. Grimsdale, and H. Sun, Adv. Opt. Mater. **4**, 746 (2016).
[15]A. K. Mandal, S. Sreejith, T. He, S. K. Maji, X. Wang, S. L. Ong, J. Joseph, H. Sun, and Y. Zhao, ACS Nano **9**, 4796 (2015).
[16]Y. Sonoda, J. Lumin. **187**, 352 (2017).
[17]H. Y. Woo, B. Liu, B. Kohler, D. Korystov, A. Mikhailovsky, and G. C. Bazan, J. Am. Chem. Soc. **127**, 14721 (2005).
[18]G. S. He, L. Tan, Q. Zheng, and P. N. Prasad, Chem. Rev. **108**, 1245 (2008).
[19]M. Sheik-Bahae, A. A. Said, T. H. Wei, D. J. Hagan, and E. W. Van Stryland, IEEE J. Quantum Electron. **26**, 760 (1990).
[20]S. Pascal, S. Denis-Quanquin, F. Appaix, A. Duperray, A. Grichine, B. L. Guennic, D. Jacquemin, J. Cuny, S. Chi, J. W. Perry, B. van der Sanden, C. Monnereau, C. Andraud, and O. Maury, Chem. Sci. **8**, 381 (2017).
[21]C. Ye, J. Zhang, X. Lin, T. Zhang, B. Wang, and T. He, Opt. Mater. Express **7**, 3529 (2017).
[22]T. He, P. C. Too, R. Chen, S. Chiba, and H. Sun, Chem. Asian J. **7**, 2090 (2012).
[23]A. Kumar, L. Li, A. Chaturvedi, J. Brzostowski, J. Chittigori, S. Pierce, L. A. Samuelson, D. Sandman, and J. Kumar, Appl. Phys. Lett. **100**, 203701 (2012).
[24]T. He, W. Hu, H. Shi, Q. Pan, G. Ma, W. Huang, Q. Fan, and X. Lin, Dyes Pigm. **123**, 218 (2015).
[25]M. Y. Berezin and S. Achilefu, Chem. Rev. **110**, 2641 (2010).